# Flow Energy Harvesting Using Piezoelectric Cantilevers with Cylindrical Extension

Xiaotong Gao, *Member, IEEE*, Wei-Heng Shih and Wan Y. Shih, *Member, IEEE*

***Abstract*— We present a new piezoelectric flow energy harvester (PFEH) based on a piezoelectric cantilever with a cylindrical extension. The flow induced vibration of the cylindrical extension causes the piezoelectric cantilever to vibrate at the natural frequency of the PFEH. The PFEH provides a low-cost, compact and scalable power source for small electronics by harvesting energy from ambient flows such as wind and water streams. Prototypes were tested in both laminar and turbulent air flows demonstrating the feasibility of the design. Turbulence excitation was found to be the dominant driving mechanism of the PFEH with additional vortex shedding excitation contribution in the *lock-in* region.**

***Index Terms*—Flow energy harvesting, Piezoelectric energy harvester, Piezoelectric cantilever, Flow induced vibration**

## I. Introduction

ENERGY harvesting technology has been explored for more than a decade as an enabling technology to power unmanned autonomous systems such as wireless sensor networks (WSNs) [1]-[4]. Flow energy is readily available both outdoors and indoors in the form of air and water streams. Miniaturized turbine systems have been investigated to convert the ambient wind energy into electricity for wireless sensors [4]-[8]. However, the disadvantages associated with the turbine systems include complexity, high fabrication and maintenance costs, and unfavorable scalability at small scale due to high viscous drag and bearing loss [9]. On the other hand, piezoelectric devices offer the potential as a flow energy harvester without electromagnetic induction. Priya et al. [10], [11] replaced the electromagnetic generator in a traditional windmill with piezoelectric bimorphs to convert wind energy into electrical energy. Taylor et al. [12] explored tapping into the vortex street created in the wake of a stationary cylinder using a piezoelectric "eel" device consisting of a soft, flexible polymeric piezoelectric strip made of polyvinylidene fluoride (PVDF) to harvest flow energy from sea current. Using a similar principle, Li et al [13] explored a "piezo-leaf" energy harvesting system where the PVDF strip of the "eel" system was replaced by a PVDF cantilever with a large triangular plastic "leaf" attached to the free end of the cantilever to improve the power generation.

As explained in detail in the following sections, we report a flow energy harvesting device consisting of a piezoelectric cantilever with a cylindrical extension. This new device is more effective and compact compared to the piezoelectric windmill, eel and leaf because it utilizes fluid forces exerted on the cylindrical extension to directly drive the piezoelectric cantilever to vibrate. The background of the behavior of a cylinder in a cross flow is introduced in Sec. II. The design and prototype testing are described in Sec. III and Sec. IV, respectively. The experimental results are demonstrated and discussed in Sec. V. Conclusions are given in Sec. VI.

## II. Background

When a cylinder is placed in a flow whose direction is perpendicular to the axis of the cylinder--hence the name of cross flow--it can vibrate in a direction normal to the flow direction. This flow induced vibration (FIV) may be caused by the turbulence generated by the flow around and in the wake of the cylinder. The turbulence represents the random fluctuations of the flow and is not periodic. The turbulence excited FIV can occur at any flow velocity with increasing amplitude with the increase of the flow velocity and a frequency around the natural frequency of the cylinder. The FIV may also be caused by the periodic vortex shedding from the cylinder's surface. When a vortex is shed from one side of the cylinder, a pressure difference forms between this side and the other side of the cylinder causing a net force exerted on the cylinder in the direction perpendicular to the flow. A vortex shed from the other side causes a force in the opposite direction. Thus the cylinder is set to vibrate due to the alternate shedding of vortices. The vortex shedding excited FIV has the same frequency as the vortex shedding which is determined as

$$f_s = SU/D \quad (1)$$

where $f_s$ is the vortex shedding frequency, $S$ the dimensionless Strouhal number, $U$ the incoming flow velocity and $D$ the

Manuscript received December 31, 2010. This work is supported by the Nanotechnology Institute, a University Grant program of the Commonwealth of Pennsylvania's Ben Franklin Technology Development Authority through Ben Franklin Technology Partners of Southeast Pennsylvania.



Xiaotong Gao is with the Department of Materials Science and Engineering, Drexel University, Philadelphia, PA 19104 USA (e-mail: gao.xiaotong27@gmail.com)

Wei-Heng Shih is with the Department of Materials Science and Engineering, Drexel University, Philadelphia, PA 19104 USA (corresponding author, phone: 215-895-6636; fax: 215-895-6760; e-mail: shihwh@drexel.edu)

Wan Y. Shih is with the School of Biomedical Engineering, Science and Health Systems, Drexel University, Philadelphia, PA 19104 USA (e-mail: shihwy@drexel.edu)

cylinder diameter. [14] When the vortex shedding frequency is close to the natural frequency of the cylinder, it will begin to lock into the cylinder's natural frequency and will stay locked in that frequency even when the flow velocity increases within a certain range. This phenomenon is termed as *lock-in* of the vortex shedding. Within the *lock-in* region, the vortex shedding frequency coincides with the natural frequency of the cylinder, essentially driving the cylinder to resonance and enhancing the vibration amplitude of the cylinder. Outside the *lock-in* region, without the resonance mechanism, the turbulence contribution is dominant. More detailed introduction of the FIV of a cylinder can be found in [14] and [15].

## III. Design

In the piezoelectric "eel" and "leaf" systems, the piezoelectric devices were placed in the wake of a stationary cylinder in a cross flow. Alternate vortices shed in the wake of the cylinder forcing the piezoelectric devices to oscillate and hence generating electricity. However, if the cylinder in a cross flow is free to vibrate and it is attached directly to a piezoelectric device, the FIVs of the vibrating cylinder can directly drive the vibration of the piezoelectric device, likely allowing more effective conversion of the flow energy to electricity. Significant flow energy can be converted to FIVs as best illustrated by the collapse of the Old Tacoma Narrows Bridge in the wind in 1940[16]. Inspired by this example, we propose to utilize the FIVs to harvest flow energy. We choose piezoelectric conversion for its low cost, high electromechanical coupling, and high energy density [17]. Due to the relatively large forces induced by the FIVs compared to those induced by vortices in "eel" and "leaf", we were able to use thicker and stiffer but higher-performance piezoelectric ceramics – lead zirconate titanate (PZT) in our design instead of PVDF which was thinner and less stiff but has a piezoelectric coefficient an order of magnitude lower than that of PZT.

The present piezoelectric flow energy harvester (PFEH) consists of a piezoelectric cantilever (PEC) with a cross-flow cylinder attached to its free end as schematically shown in Fig. 1(a). Since the cross-flow cylinder is at the free end of the PEC, it is free to vibrate to respond to the fluid forces generated by the flow on the cylinder, and in turn the PEC will vibrate with the cylinder to generate electricity. This design is scalable and, compared to other flow energy harvesters using piezoelectric devices [10]-[13], simpler and more compact thus easier to be miniaturized and integrated with small electronics. Without rotary components, the maintenance cost is much reduced.

During the reviewing process of this paper, Sirohi and Mahadik [18] also published a wind energy harvester based on piezoelectric cantilevers with a bluff. But, the construction of their wind energy harvester was more complicated and different from the PFEH as they used two cantilever beams and oriented the triangular bar bluff perpendicular to the cantilever beams, whereas the PFEH consisted only one cantilever beam and the circular bluff of the present PFEH was oriented parallel to the cantilever beam.

## IV. Experiments

Three PFEHs were constructed and tested as listed in Table I. In all PFEHs, the PECs were comprised of a 127μm-thick lead zirconate titanate (PZT) layer (T105-H4E-602, PIEZO SYSTEMS INC., Cambridge, MA) and a 75μm-thick stainless steel (SS) layer (type 304, Trinity Brand Industries, Inc., Countryside, IL). The PZT and SS layers were bonded together by an epoxy layer. The length and width of the PECs were 31 mm and 10 mm, respectively. The cylinders were made of 0.2mm-thick photo paper and hollow so that they were lightweight. The lengths of the cylinders were all 36 mm but three different diameters (11.6 mm, 18.4 mm and 29.1 mm, see Table I) were examined. The cylinders were attached to the free ends of the PECs by using epoxy as schematically shown in Fig. 1(a). Thus the total length of the PFEHs was 67 mm. The PFEHs were tested in both laminar flows generated by a Flotek-1440 wind tunnel (GDJ Inc., Mentor, OH) and turbulent flows generated by an electric fan. The photographs of the experimental setups were shown in Figs. 1(b) and 1(c).

Table I. Properties of the PFEHs. All the PFEHs have the same cantilever dimension of 31×10 mm and cylinder length of 36 mm.

| | Cylinder diameter, $D$ (mm) | Natural frequency, $f_0$ (Hz) | Capacitance, $C$(nF) | Optimal Load, $R_{opt}$(kΩ) | $U_m/f_0D$ |
|---|---|---|---|---|---|
| PFEH-A | 11.6 | 43.1 | 62 | 60 | 9.0 |
| PFEH-B | 18.4 | 30.7 | 64 | 81 | 8.7 |
| PFEH-C | 29.1 | 20.7 | 62 | 124 | 8.9 |

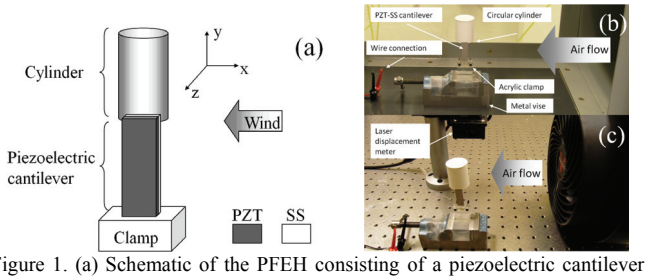


Figure 1. (a) Schematic of the PFEH consisting of a piezoelectric cantilever with a circular cylinder attached to the free end in a cross-flow (not to scale). (b) The experimental setup within the chamber of a Flotek-1440 wind tunnel. (c) The experimental setup using an electric fan.

## V. Results and Discussion

In a laminar flow inside the wind tunnel, the PFEH vibrated visibly perpendicular to the flow, which induced an oscillating piezoelectric voltage across the PZT layer measured by an Agilent 54845A oscilloscope (Agilent, Palo Alto, CA). Although we could not measure the vibration amplitude of the PFEH directly in the wind tunnel due to space limitation, we were able to measure both the vibration amplitude and the induced voltage in a fan test which showed that the induced voltage was proportional to the vibration amplitude of the PFEH as shown in the insert of Fig. 2(a) for example. Thus the induced voltage will be used as an indicator of the vibration amplitude in the following discussion. In the experiment, although the induced voltage fluctuated with time, the average amplitude of the induced voltage over a long period of time (>1

min) remained stable. Figure 2(a) shows the average amplitude of the open-circuit (OC) induced voltage, $V_{OC}$, over a period of 2 minutes versus the wind velocity. As can be seen, for the three PFEHs, the $V_{OC}$ increased with the wind velocity and the cylinder diameter. In Fig. 2(a), we also included the $V_{OC}$ of a 31×10 mm and a 67×10 mm PECs both without a cylinder. The latter had a length equal to the total length of the PFEHs. For the two PECs without a cylinder, little $V_{OC}$ was generated even at high wind velocities. This confirms that the PFEHs were driven by the FIVs induced by the cylinder extensions.

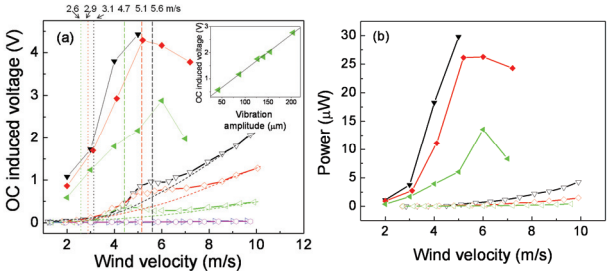


Figure 2. (a) Open-circuit (OC) induced voltage and (b) power output of PFEH-A (◁/◀),PFEH-B (◇/◆), PFEH-C (▽/▼), a 31×10mm PEC without a cylinder (▷) and a 67×10mm PEC without a cylinder (○). The open and solid symbols represent data in the wind tunnel test (laminar flow) and the fan test (turbulent), respectively. The insert in (a) shows the OC induced voltage versus the displacement measured at the mid-point of the cylinder in PFEH-A.

The Reynolds number, $R_e$, is defined as $R_e = \rho UD/\mu$ where $\rho$ the mass density of the air (1.2 kg/m$^3$ as an average quantity since it depends on the temperature, shape and material of the cylinder), $U$ the wind velocity, $D$ the cylinder diameter and $\mu$ the absolute viscosity of the air ($18.27\times10^{-6}$ Pa·s at 291.15 °K). In this work, the calculated $R_e$ was between 2000 and 19000. Within this $R_e$ range, the vortex flow in the wake of the cylinder is turbulent [15]. This turbulent wake flow can cause the PFEHs to vibrate at its natural frequency. As the wind velocity increases, the strength of the turbulent wake flow also increases resulting in the increase of induced voltage as shown in Fig.2 (a). That the induced voltage was due to turbulence excitation is also supported by the time history and power spectral density (PSD) of the $V_{OC}$ as shown in Figs. 3(a) and (b), respectively. As can be seen in Fig. 3(a), the $V_{OC}$ of the PFEH-C had an amplitude that changed randomly with time indicating the PFEH-C was oscillating due to the random forces generated by the turbulent wake flow. Furthermore, by examining the PSDs of the $V_{OC}$ in Fig. 3(a), it was found that the frequency of the oscillating $V_{OC}$ was the natural frequency of the PFEH-C (see Fig. 3(b)), which remained true for all wind velocities examined and for all three different cylinder diameters.

It can also be seen in Fig. 2(a) that the induced voltage curves in the wind tunnel test had humps over certain ranges of wind velocity. These humps were thought to be due to the *lock-in* phenomenon of the vortex shedding as discussed in Sec. II. Using Eq. (1), the on-set wind velocity of the *lock-in* can be calculated by replacing the vortex shedding frequency, $f_s$, with the natural frequency of the PFEH, $f_0$, and using a Strouhal number of 0.2 which is constant in the range of the Reynolds number in this work [14], and the cylinder diameter listed in Table I. The calculated on-set wind velocities were 2.6, 2.9 and 3.1 m/s for PFEH-A, PFEH-B and PFEH-C, respectively, as indicated in Fig. 2(a). As can be seen, the humps started approximately from these wind velocities. Within the hump or *lock-in* region, the PFEH was at resonance as the frequency of the vortex shedding matched the natural frequency of the PFEH, giving rise to an enhanced induced voltage. Note that, in the *lock-in* region, both the turbulence excitation and the vortex shedding excitation contributed to the vibrations of the PFEH. However, because both gave rise to vibrations at the natural frequency of the PFEH, they were not differentiable on the PSD of the $V_{OC}$ as shown in Fig. 3(b).

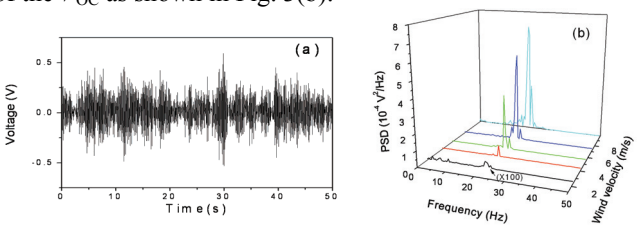


Figure 3. (a) Time-history of the open-circuit (OC) induced voltage of the PFEH-C at 4.4m/s wind velocity and (b) power spectral density (PSD) of the OC induced voltage of PFEH-C at different wind velocities in the wind tunnel test. The PSD at 2.6 m/s wind velocity was amplified 100 times to make the peak visible in the plot.

It was found that in the wind tunnel test the wind velocity at the center of the *lock-in* region, $U_m$, is proportional to the natural frequency of the PFEH, $f_0$, and the cylinder diameter, $D$. From Fig. 2(a), the $U_m$ was 4.7, 5.1 and 5.6 m/s for 11.6, 18.4 and 29.1 mm cylinder diameters, respectively. With these data and the natural frequencies listed in Table I, it can be calculated that $U_m \approx 9 f_0 D$ for all three PFEHs as shown in Table I. With this empirical relationship, one can design the PFEH to work at its strongest resonance at the prevailing wind velocity in the environment. More study will be performed in the future to examine if this relationship holds when other parameters are changed, such as the cantilever dimension, cylinder geometry and materials.

An electric fan was used to generate turbulent flows that mimic the natural wind as shown in Fig. 1(c). The flow velocity was measured by using a windmill anemometer (LA CROSSE® Technology). A laser displacement meter was used to measure the vibration amplitude at the mid-point of the cylinder. The $V_{OC}$ of the PFEHs in the fan test were shown in Fig. 2(a) as solid symbols. As can be seen, the $V_{OC}$ in the fan test were much larger than those in the wind tunnel test presumably due to the presence of the turbulence in the flow [15]. It can be seen that the humps due to *lock-in* also appeared in the fan test but the wind velocities at which the *lock-in* occurred differed from those in the wind tunnel test. In the fan test, the highest wind velocity was 7 m/s because of the limitation of the fan power.

To draw electric power from the PFEHs, we connected resistive loads to the PZT layers. The matching load resistance, $R_{opt}$, for maximum power generation can be calculated as $R_{opt}=1/(2\pi f_0 C)$ where $C$ is the capacitance of the PZT layer [10]. The calculated matching load resistances were listed in Table I.

The power output from the PFEHs connected with the matching load resistances were plotted versus the wind velocity in Fig. 2 (b). As can be seen, the power output increased with the wind velocity and cylinder diameter. And, higher power was obtained in the fan test than in the wind tunnel test. Up to 30 μW was obtained with the PFEH-C at 5 m/s wind velocity in the fan test. To be precise, the $R_{opt}$ should be obtained by measuring the rms induced voltage and power as a function of load resistance. We have done comparison of the maximum power obtained from the calculated $R_{opt}$ and that obtained from measured rms voltage and found that the two powers were similar. Therefore, it is convenient to use the calculated $R_{opt}$ as shown above. Note that the above power output is un-rectified AC power consumed by a resistive load directly connected to the PFEH. With a properly designed rectifying and control circuit, the PFEH can output DC power which can be higher than the AC power by a factor of 3 to charge a battery or capacitor. [19]

## VI. Conclusion

In summary, we reported a PFEH consisting of a piezoelectric cantilever with a cylindrical extension. The interaction between the cylindrical extension and ambient flow drove the piezoelectric cantilever to vibrate and generate electricity. The PFEH provides a low cost, compact and scalable power solution for small electronics by harvesting energy from ambient flows such as wind or water stream. Prototype PFEHs were constructed and tested in both laminar and turbulent air flows demonstrating the feasibility of the design. The PFEHs generated higher voltage and power in the turbulent flow than in the laminar flow. It was found that turbulence excitation was the dominant driving mechanism of the PFEH with additional contribution from vortex shedding excitation in the *lock-in* region. The frequency of the induced voltage remained at the natural frequency of the PFEH at any wind velocity which can help simplify the design of the external circuit. As a demonstration of the practical application of the PFEH, a 58×10 mm bimorph PEC with a cylindrical extension of 36 mm in length and 29.1 mm in diameter incorporating with an EH-300 energy harvesting module (Advanced Linear Devices Inc.) was shown to successfully generate power to continuously operate a MCP9700 thermometer (Microchip Inc.) in a 5.2 m/s wind generated by the fan.

In the future work, a CFD (Computational Fluid Dynamics) model of the PFEH will be developed to investigate the performance and operating parameters of the PFEH.

## Acknowledgment

The work was supported in part by the Nanotechnology Institute (NTI) of Benjamin Franklin Partnership of southeastern Pennsylvania. The authors would also like to thank Bakhtier Farouk for helpful discussions.

## References

[1] J.A. Paradiso and T. Starner, “Energy scavenging for mobile and wireless electronics.” *IEEE Pervasive Computing*, vol. 4, pp. 18-27, Jan. 2005.

[2] R. Bogue, “Energy harvesting and wireless sensors: a review of recent developments,” *Sensor Review,* vol. 29, pp. 194-202, July 2009.

[3] A. Khaligh, P. Zeng and C. Zheng, “Kinetic energy harvesting using piezoelectric and electromagnetic technologies – s*tate of the art”, IEEE Transactions on Industrial Electronics*, vol. 57, no. 3, pp. 850-860, March 2010.

[4] D. Rancourt, “Evaluation of Centimeter-Scale Micro Wind Mills:Aerodynamics and Electromagnetic Power Generation.” in *PowerMEMS, Freiburg, Germany*, 2007, pp. 93-96.

[5] A. Bansal,D. A. Howey and A. S. Holmes, "CM-SCALE AIR TURBINE AND GENERATOR FOR ENERGY HARVESTING FROM LOW-SPEED FLOWS," presented at the Transducers, Denver, CO, USA, June 21-25, 2009.

[6] M.A. Weimer, T.S. Paing and R.A. Zane, “Remote area wind energy harvesting for low-power autonomous sensors," in *Power Electronics Specialists Conference, 2006. PESC '06. 37th IEEE*, 2006, pp. 1-5.

[7] A. S. Holmes, G. Hong, K. R. Pullen and K. R. Buffard, "Axial-flow microturbine with electromagnetic generator: design, CFD simulation, and prototype demonstration," in *Micro Electro Mechanical Systems, 2004. 17th IEEE International Conference on. (MEMS)*, 2004, pp. 568-571.

[8] C. C. Federspiel and J. Chen, “Air-powered sensor,” in *Sensors, Proceedings of IEEE,* vol. 21, pp. 22-25, Jan. 2003.

[9] P. D. Mitcheson, E. M. Yeatman, G. K. Rao, A. S. Holmes and T. C. Green, “Energy harvesting from human and machine motion for wireless electronic devices,” *Proceedings of the IEEE*, vol. 96, pp. 1457-1486, Sept. 2008.

[10] S. Priya, C. T. Chen, D. Fye and J. Zahnd, “Piezoelectric windmill: A novel solution to remote sensing,” *Jpn. J. Appl. Phys. Part 2 - Lett. Express Lett*. vol. 44, pp. L104-L107, Dec. 2005.

[11] S. Priya, “Modeling of electric energy harvesting using piezoelectric windmill,” *Applied Physics Letters*, vol. 87, no. 18, pp. 184101-184101-3, Oct. 2005.

[12] G. W. Taylor, J. R. Burns, S. M. Kammann, W. B. Powers and T. R. Welsh, “The energy harvesting eel: A small subsurface ocean/river power generator,” *IEEE Journal of Oceanic Engineering*, vol. 26, pp. 539-547, Oct. 2001.

[13] S. Li and H. Lipson, “Vertical-stalk flaping-leaf generator for wind energy harvesting,” in *ASME 2009 Conference on Smart Materials, Adaptive Structures and Intelligent Systems*, Oxnard, CA, Sept. 20-24, 2009.

[14] R. D. Blevins, *Flow-induced vibration*, Van Nostrand Reinhold Co., 1977.

[15] S.-S. Chen, Flow-induced vibration of circular cylnidrical structures, Hemisphere publishing corporation, 1987.

[16] K. Y. Billah and R. H. Scanlan, “Resonance, Tacoma Narrows Bridge Failure, and Undergraduate Physics Textbooks,” *American Journal of Physics*, vol. 59, pp. 118-124, Feb. 1991.

[17] S. Priya, “Advances in energy harvesting using low profile piezoelectric transducers,” *Journal of Electroceramics*, vol. 19, pp. 165-182, Sept. 2007.

[18] J. Sirohi and R. Mahadik, “PiezoelectricWind Energy Harvester for Low-Power Sensors,” *Journal of Intelligent Material Systems and Structures*, vol. 22, no. 18, pp. 2215-2228, Dec. 2011.

[19] G. K. Ottman, H. F. Hofmann, and G. A. Lesieutre, “Optimized piezoelectric energy harvesting circuit using step-down converter in discontinuous conduction mode,” *IEEE Trans. Power Electron*., vol. 18, no. 2, pp. 696–703, Mar. 2003.